Electronic transport properties in amorphous and crystalline $FeZr_2$ examined via the density of states

M. Dikeakos,[1,2,*] Z. Altounian,[1] and M. Fradkin[1,†]
[1]*Centre for the Physics of Materials and Department of Physics, McGill University, 3600 University Street, Montréal, Québec H3A 2T8, Canada*
[2]*IMI, National Research Council Canada, 75 de Mortagne Boulevard, Boucherville, Québec J4B 6Y4, Canada*
(Received 4 November 2003; revised manuscript received 9 March 2004; published 23 July 2004)

An extensive study of $FeZr_2$ was undertaken in order to gain insight into the amorphous structure of the glass and the metastable "big-cube" structure of the intermediate crystallization product. Examination of the temperature dependence of the resistivity (ρ) revealed a large ρ and negative temperature coefficient of ρ (α_ρ) for the glass, which is not unexpected. However, an even larger ρ and negative α_ρ observed for the *cF*96 big cube is quite unexpected for the crystalline structure in this temperature range. Through tight-binding–linear muffin tin orbital–atomic spheres approximation density of states calculations, it is shown that $s-d$ scattering is the reason for the high ρ and negative α_ρ in the big cube, and therefore, $s-d$ scattering accounts for the high ρ and negative α_ρ in transition-metal–transition-metal glasses.

DOI: 10.1103/PhysRevB.70.024209 PACS number(s): 71.20.−b, 71.23.−k, 72.15.−v

I. INTRODUCTION

The increasing interest of late in nanostructured materials, some of which are produced from partial or full crystallization of the glassy/amorphous solid,[1,3] requires a better knowledge of the amorphous state in order to fully realize the potential of such materials. In recent years, scientific effort has been focused on understanding the electronic band structure and the structure of metallic glasses at the atomic scale.[1,2,4–7] Whereas data on the electronic density of states can provide a satisfactory explanation of physical properties, such as resistivity, superconductivity, and magnetism, knowledge of the atomic arrangements is required to better comprehend the mechanical and metallurgical characteristics of these glasses, such as hardness, strength, and their behavior under thermal and mechanical treatments below the crystallization temperature. Given the atomic disorder of glasses, such information is not obtained easily.[2,7]

Metal-metal binary glasses based on zirconium are ideal for the systematic examination of the effect of an amorphous structure on physical properties given their combination of stability over an extensive range of composition and great variety of properties. In amorphous $FeZr_2$, crystallization proceeds from the evolution of a large number of very small crystallites (2.0–3.0 nm)—as attested to by transmission electron microscope micrographs taken just after the first exothermal event, observed in a differential scanning calorimeter (DSC), corresponding to the first crystallization product, the metastable *cF*96 structure.[8] The formation of the *cF*96 phase brings about an increase in electrical resistivity (ρ) over that in the glassy state. The grain-boundary resistance due to the numerous small crystallites is not responsible for the increase since annealing at 900 K for 2 h results in grain growth ($\sim 1\ \mu$m in size), but no decrease in resistivity.[8] The high resistivity of the *cF*96 phase is an intrinsic property. Unlike the stable *tI*12 phase of the final crystallization product, both the metastable *cF*96 phase of the first crystallization product and the glassy state exhibit a negative temperature coefficient of resistivity (α_ρ).[8–10] Although a negative α_ρ over the whole temperature range has recently also been observed in some ternary quasicrystals and their approximants,[11–13] in the case of quasicrystals and their approximants, there is speculation that the negative α_ρ is critically dependent on microstructure[14] and that it is due to partial chemical disorder.[13] However, unlike the ternary quasiscrystal systems, the $FeZr_2$ binary is a stoichiometric compound with a narrow single-phase region and well-defined atomic positions. The question here is as follows: To what differences in the two crystalline structures of the $FeZr_2$ binary can this be attributed? What is special about the 96-atom cubic cell structure (the "big cube," as it is commonly called)? An answer to this question may shed some light on the parent amorphous structure itself, given the prevalent belief that the short-range order of the metastable state is similar to that of the glassy state.

Because of the well-characterized crystal structure of the big cube, unlike the quasicrystals and their approximants, a look at the density of states (DOS) may provide some clues. In order to explain the difference in the sign of the temperature coefficient of resistivity for the two crystalline structures (*cF*96 and *tI*12) of $FeZr_2$, changes in the DOS with temperature is examined. Results of such DOS calculations performed using a tight-binding–linear muffin tin orbital–atomic spheres approximation formalism (TB-LMTO-ASA) are presented in this work.

II. EXPERIMENTAL METHODS

The binary $FeZr_2$ alloy was prepared by arc-melting appropriate amounts of the constituent elements—Fe 99.9% and Zr 99.95%—under titanium-gettered high-purity (99.995%) argon gas. Small pieces of the resulting ingots were melt-spun under a 17-kPa high-purity He atmosphere onto the surface of a rotating copper wheel with a tangential speed of 50 m/s.

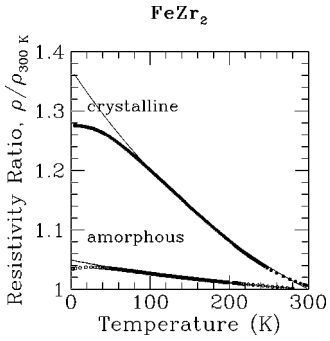

FIG. 1. Plots of the temperature dependence of the resistivity (ρ) for amorphous and crystalline $FeZr_2$. The solid lines are a least-squares fit of Mizutani's empirical relation (Ref. 16) $\rho(T)/\rho(300\ \mathrm{K}) = A + B\exp(-T/\Delta_T)$ to the data.

Elemental composition and homogeneity of the samples were verified by electron microprobe spectroscopy. Analysis at several positions along the ribbon samples showed that the samples were homogeneous with the concentration of each constituent element differing from the expected nominal amount by less than 1 at.%. The structural state of the samples was examined by graphite-monochromated Cu K_α x-ray diffraction (XRD) on a conventional automated powder diffractometer. Samples were judged to be amorphous based on the absence of sharp diffraction peaks. XRD of the crystalline products exhibited Bragg peaks that were somewhat broadened by thermal and zero-point motion, small crystallite size, and strain. Nevertheless, they were well defined (*cF*96 or *tI*12) and could not be mistaken for the broad peaks observed for amorphous material.

Crystalline samples of the binary alloy were obtained by heating the glassy ribbons in a Perkin Elmer Pyris 1 DSC under a high-purity (99.995%) argon gas flow at a heating rate of 20 K/min to a temperature just past the point of crystallization T_x.

Changes in resistance with temperature (in the range between 1.6–300 K) for both the glassy and crystalline states of the $FeZr_2$ binary alloy were examined using a four-terminal ac bridge technique in conjunction with a helium-based cryostat. A sensitivity of 10^{-5} Ω was easily achieved with this setup.

III. RESULTS AND DISCUSSION

A. Low-temperature resistivity measurements

Owing to the sensitivity of the electrical resistance of a material to variations in the electronic configuration of the underlying atomic structure, the behavior of the resistance offers yet another means of characterizing the glassy and metastable crystalline states of the $FeZr_2$ binary. To this end, resistivity measurements from room temperature down to below 4 K were taken for the amorphous and crystalline samples. A plot of the temperature dependence of the resistivity for amorphous and crystalline $FeZr_2$ is given in Fig. 1. The maximum in $\rho(T)$ at temperatures below 40 K is due to the scattering of the conduction electrons from the localized spin fluctuations (characteristic of nearly magnetic systems).[15] The downward turn of the maximum as T decreases is due to the onset of superconductivity. For *a*-$FeZr_2$, $\rho(300\ \mathrm{K})$ is $165\pm5\ \mu\Omega$ cm, which is greater than that of the stable tetragonal state ($115\pm10\ \mu\Omega$ cm), but less than that of the metastable big cube ($215\pm10\ \mu\Omega$ cm).[8–10,19]

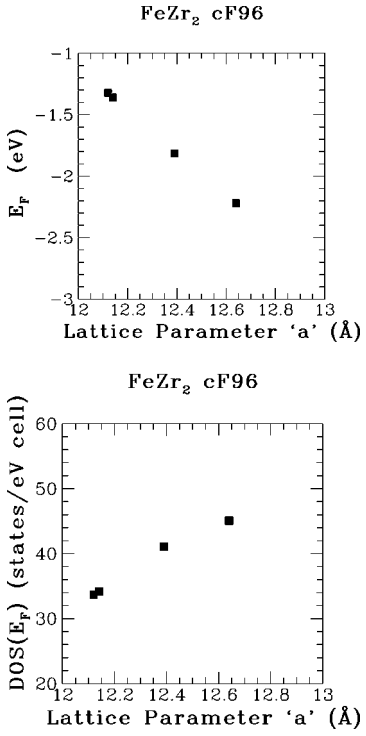

FIG. 2. The Fermi energy, E_F, and density of states at the Fermi level, DOS(E_F), plotted against the lattice parameter *a* for *cF*96 *c*-$FeZr_2$. The values of E_F and DOS(E_F) were calculated using the TB-LMTO-ASA method of Andersen *et al.* (Ref. 20). For the formalism used here, E_F is measured from the bottom of the conduction band. (The size of the points is indicative of the errors.)

A straightforward and most common way of characterizing all types of material is through the temperature coefficient of resistivity, α_ρ. It will be used here to look for similarities between the glassy and metastable crystalline phases. For *a*-$FeZr_2$, α_ρ was found to be $(-12.5\pm2.0)\times10^{-5}\ \mathrm{K}^{-1}$. A negative α_ρ is consistent with that of other transition metal-transition metal glasses.[17,18] However, α_ρ is known to be negative for the metastable cubic *cF*96 state $[(-100\pm10.0)\times10^{-5}\ \mathrm{K}^{-1}]$ and positive for the equilibrium tetragonal *tI*12 state $[(125\pm15.0)\times10^{-5}\ \mathrm{K}^{-1}]$.[8,9,19] This behavior of the resistivity is atypical of most crystals and strongly suggests the possibility that the amorphous and crystalline systems share a common scattering mechanism; this unexpected behavior points to a similarity in the local order in both phases.

B. Density of states

The main difficulties in the calculations of the electronic structure of amorphous metals arise from the fact that these metals are disordered systems characterized by a lack of long-range order of atoms and consequently the usual band theory is inapplicable. Because significant DOS information

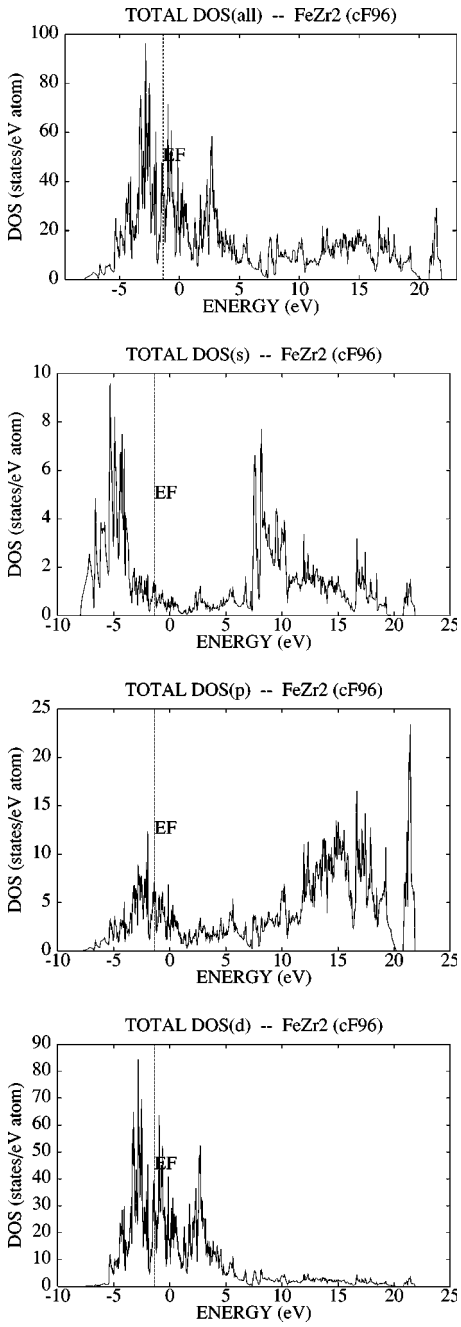

FIG. 3. Total densities of states (DOS) for the *cF*96 structure of *c*-$FeZr_2$ calculated using the TB-LMTO-ASA method of Andersen *et al.* (Ref. 20). For the formalism used here, E_F is measured from the bottom of the conduction band.

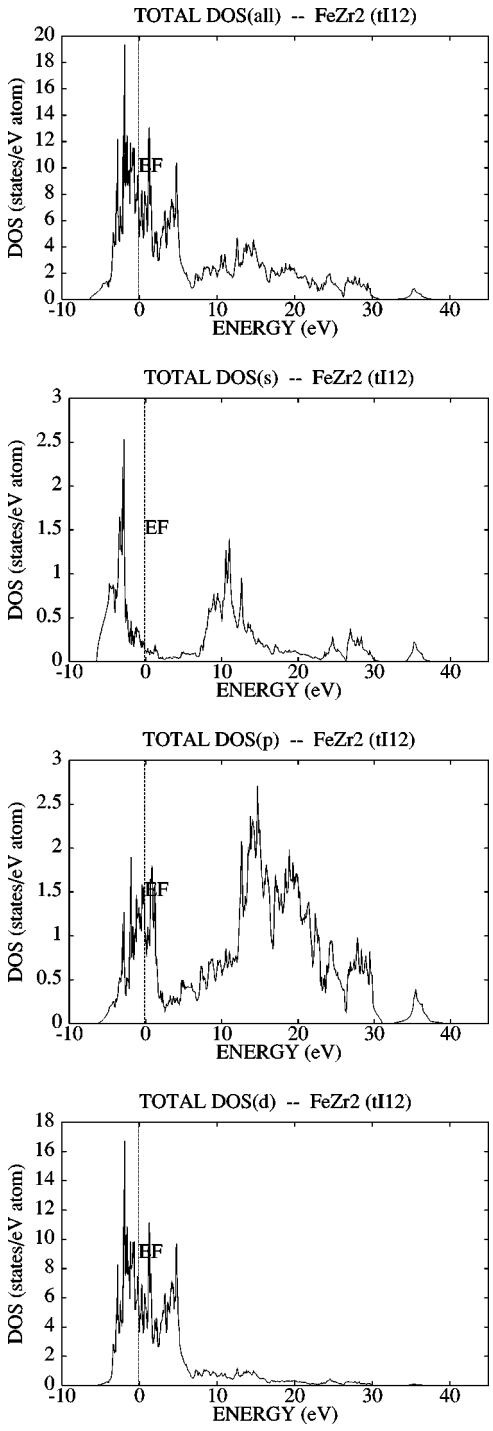

FIG. 4. Total densities of states (DOS) for the *tI*12 structure of *c*-$FeZr_2$ calculated using the TB-LMTO-ASA method of Andersen *et al.* (Ref. 20). For the formalism used here, E_F is measured from the bottom of the conduction band.

on the glassy state of $FeZr_2$ is difficult to come by, special focus is placed here on the crystalline states of $FeZr_2$, namely *cF*96 and *tI*12. The desire is to gain insight into the *cF*96 structure that is formed as the first crystallization product from the glassy state. In particular, the hope is to discover differences in the density of states (and its behavior) of the metastable cubic and equilibrium tetragonal states, which may explain the larger resistivity as well as the negative temperature coefficient of the *cF*96 state. Subsequently, given the belief that the metastable state shares a common short-range order with the glassy state, some information on the amorphous structure may be inferred.

To start, the effect of contraction and/or expansion of the *cF*96 lattice structure on the total density of states at the Fermi energy was examined. (For the formalism used here, E_F is measured from the bottom of the conduction band.) In Fig. 2, the DOS at E_F is seen to decrease linearly with de-

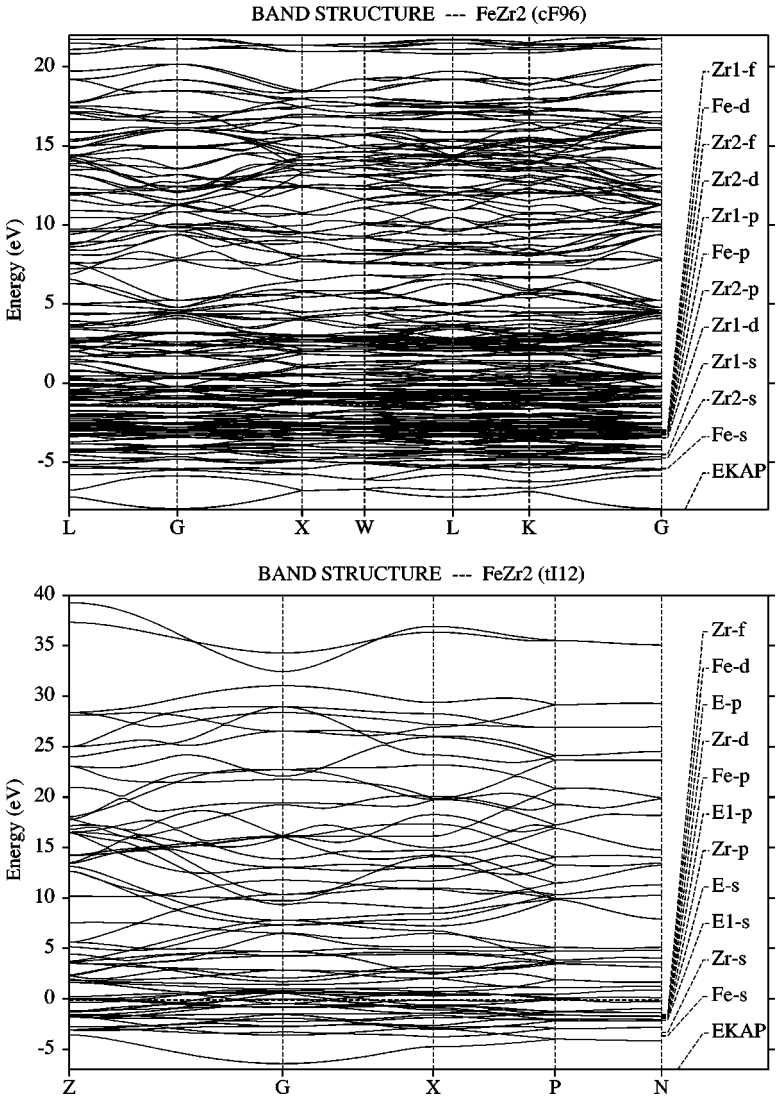

FIG. 5. Band structure of *cF*96 and *tI*12 *c*-$FeZr_2$ calculated using the TB-LMTO-ASA method of Andersen *et al.* (Ref. 20). Note the low-lying state—the Zr1 *d* band which lies just above the *s* states in the *cF*96 structure. (For the formalism used here, E_F is measured from the bottom of the conduction band.)

creasing lattice parameter "a," i.e., the lattice contracts. At the same time, E_F is seen to increase with decreasing lattice parameter consistent with metallic behavior. Transition metals are characterized by a tightly bound *d* band that overlaps and "hybridizes or mixes" with a broader nearly-free-electron *sp* band. Hybridization or mixing of valence states in an atom occurs when the states are fairly close in energy. The relative separation of the valence *s* and *d* energy levels increases in going down a column of the Periodic Table from 3*d* to 4*d* away from the left-hand side of the transition-metal series. This behavioral difference between the valence *sp* band and *d* electrons arises from the *d* level lying inside the outer *s* level, which leads to a small overlap between the *d* orbitals in the bulk. Transition-metal *sp* valence electrons are found to be scattered very little by the lattice. On the other hand, transition-metal *d* electrons are strongly scattered. As the structure contracts, the bonding between atoms increases, the center of gravity of the *d* band moves up under compression as the electronic charge is confined into yet smaller Wigner-Seitz sphere volumes, and the energy of the Fermi level increases.

Electronic band calculations for the *cF*96 and *tI*12 structures of *c*-$FeZr_2$ were performed using the TB-LMTO-ASA method of Tank *et al.*,[20] Andersen, Jepsen, and Sob,[21] and Anderson.[22] Plots of the results are given in Figs. 3–5. (Additional DOS plots are given in Ref. 10.) A summary of the calculated DOS_{E_F} and E_F is provided in Table I. A close look at the two structures reveals two obvious differences: (i) the total DOS at E_F for *cF*96 is nearly five times that for *tI*12 and (ii) the E_F of *cF*96 is almost ten times lower than that for *tI*12. Furthermore, the contribution to the density of states at the Fermi level of Zr versus that of Fe is almost double in *cF*96 and practically even for *tI*12, i.e., PDOS(Zr): PDOS(Fe) (PDOS stands for partial density of states) is 1.7:1 for *cF*96 and 1.2:1 for *tI*12. However, the ratio of the Fe *d* states to that of the Zr *s* states at E_F in *cF*96 is less than half that in *tI*12, i.e., PDOS(Fe *d*): PDOS(Zr *s*) is 11:1 in *cF*96 and 25:1 in *tI*12. One other observation is of an unexpected low-lying state—the *d* state of Zr1 in *cF*96 lies just above the valence *s* states. All of this leads to the conclusion that the (experimentally observed) resistivity is larger for *cF*96 than for *tI*12 owing to an increase in *s*-*d* mixing (*s*-*d* hybridization) in the metastable cubic state. This in turn confirms the earlier observation that the large ρ of *cF*96 is not brought about by the grain-boundary resistance associated with the presence of small crystallites, but is indeed intrinsic

TABLE I. Total and partial densities of states and Fermi energies calculated for different lattice parameters of the *cF*96 and *tI*12 structures of *c*-$FeZr_2$. The uncertainty is less than 2% for the DOS values and of the order of 0.5% for the E_F.

c-$FeZr_2$		*cF*96		*tI*12	
Lattice	*a*	12.14	12.12	6.385	6.378
(Å)	*c*			5.596	5.589
	all	33.08	34.00	7.35	6.55
Total DOS_{E_F}	*s*	1.09	1.10	0.16	0.16
(states/eV atom)	*p*	5.36	5.69	1.21	1.19
	d	26.64	27.18	5.98	5.20
$PDOS_{E_F}$(Fe)	*s*	0.15	0.17	0.05	0.05
(states/eV atom)	*p*	1.92	2.10	0.55	0.54
	d	10.19	10.09	2.69	2.54
$PDOS_{E_F}$(Zr1)	*s*	0.17	0.18	0.11	0.10
(states/eV atom)	*p*	1.16	1.26	0.66	0.65
	d	2.50	2.53	3.33	2.66
$PDOS_{E_F}$(Zr2)	*s*	0.76	0.75		
(states/eV atom)	*p*	2.29	2.33		
	d	13.95	14.56		
E_F		−1.361	−1.323	−0.122	−0.095
(eV)					

to the structure. Therefore, if the short-range order of the metastable "big cube" is similar to that of the glass (as is the belief) then the large ρ observed for the glass may also be ascribed to substantial *s*-*d* mixing. Earlier studies of the resistivity of *c*-$FeZr_2$ show relative ρ values for the glassy, metastable cubic, and equilibrium tetragonal structures to be 1:1.3:0.7, respectively.[19] It is perhaps worth noting that the ratio $\rho(cF96):\rho(tI12)$, which is 1.9:1, is fairly equal to the ratio $[\mathrm{PDOS\,(Zr)}:\mathrm{PDOS\,(Fe)}]_{cF96}:[\mathrm{PDOS\,(Zr)}:\mathrm{PDOS\,(Fe)}]_{tI12}$, which is 1.7:1.2.

Next, in order to explain the difference in sign of the temperature coefficient of resistivity for the two structures, it is necessary to examine the changes in the DOS as the temperature changes. Because all of the calculations are actually performed for $T=0$ K, temperature changes were mimicked through contraction and/or expansion of the lattice. The justification for this lies in the fact that a negative α_ρ cannot be attributed to electron-phonon scattering. Thus the contribution of the electron-phonon interaction to ρ at $T>0$ K can be ignored when simply looking for changes in the DOS that cannot be ascribed to this interaction. Physically probable lattice parameters were estimated using the coefficient of linear thermal expansion for Zr with a 200 K change in temperature. At first glance, the results in Table I reveal the answer. As the temperatures drops, the lattice contracts, E_F is raised, and the total density of states *increases* for *cF*96, but *decreases* for *tI*12. The "temperature coefficient of the total DOS at E_F" (i.e., $\Delta\mathrm{DOS}/\mathrm{DOS}$) is −0.04 and +0.07 for *cF*96 and *tI*12, respectively. Also, whereas all the PDOS for *tI*12 decrease as the temperature decreases, not all of the PDOS for *cF*96 increase; the PDOS(Fe *d*) and PDOS(Zr *s*) actually decrease. This is consistent with the picture of an increase in *s*-*d* hybridization of the Fe 3*d* and Zr 4*s* states as the temperature is lowered, and the lattice contracts. The relative values of the experimental α_ρ for the metastable cubic and equilibrium tetragonal states are, respectively, −1:1.25.[19] They are in quite good agreement with the calculated "temperature coefficient of DOS," −1:1.75.

Confirmation of the inferred DOS results for the glassy state would be of value (and could be inspiration for future work), providing further proof of the common local structure of the glass and metastable "big cube." Nevertheless, it has been possible to demonstrate from this work that *s*-*d* scattering is the reason for the high resistivities and the negative temperature coefficient of ρ in the "big cube," and therefore *s*-*d* scattering is the reason for the high ρ and negative α_ρ in TM-TM metallic glasses. Moreover, *s*-*d* scattering could be the origin of the Mooij correlation[23] observed in transition-metal–metal glasses.

IV. CONCLUSIONS

From the onset of this work, the goal was to gain some insight into the glassy structure and the mechanism involved in its crystallization. As such, a simple binary system, $FeZr_2$ was chosen for study. The choice of this system was based on the ease of formation of the glass phase and the intriguing intermediate metastable phase, the big-cube *cF*96 structure, upon crystallization to the final equilibrium tetragonal state, *tI*12.

Measurements of the temperature dependence of the resistivity exhibit the characteristic negative temperature coefficient of resistivity for both the glassy and metastable "big cube" states in contrast to the positive value for the equilibrium tetragonal state. DOS calculations revealed an increase in the total density of states at the Fermi level for the metastable structure, but a decrease in the DOS at E_F for the equilibrium tetragonal structure as the temperature decreases (i.e., as the lattice contracts), which can account for the positive α_ρ (i.e., the increase in ρ as the temperature decreases) observed in the metastable "big cube" and in the glass, insofar as their short-range order is believed similar. The contribution to the DOS at E_F of the Zr atoms as compared to that of the Fe atoms is double for the *cF*96 structure compared to an even contribution for the *tI*12 structure. This results in an increase in $s-d$ mixing for *cF*96, which would then explain the large resistance observed for the metastable state (compared with that of the equilibrium state).

The subtle complexities of the problem of characterizing the amorphous state has also been made obvious. The task is not a simple one, often being tackled in a heuristic manner.

ACKNOWLEDGMENTS

This work was supported by grants from the Natural Sciences and Engineering Research Council of Canada (NSERC) and the Fonds pour la Formation de Chercheurs et l'Aide à la Recherche, Québec.

*Author to whom correspondence should be sent. Electronic address: dikeakos@physics.mcgill.ca
†On leave from the Institute of Crystallography, Russian Academy of Science, Moscow 117333, Russia.

[1] Er. Girt, Kannan M. Krishnan, G. Thomas, Z. Altounian, and M. Dikeakos, J. Appl. Phys. **88**, 5311 (2000).
[2] X. Wang, M. Qi, and C. Dong, J. Non-Cryst. Solids **318**, 142 (2003).
[3] N. X. Sun, K. Zhang, X. H. Zhang, X. D. Liu, and K. Lu, Nanostruct. Mater. **7**, 637 (1996).
[4] P. Oelhafen, R. Lapka, U. Gubler, J. Krieg, A. DasGupta, H.-J. Güntherodt, T. Mizoguchi, C. Hague, J. Kübler, and S. R. Nagel, *Proceedings of the 4th International Conference on Rapidly Quenched Metals, Volume II*, edited by T. Masumoto and K. Suzuki (Japan Institute of Metals, Sendai, 1982), p. 1259.
[5] Ian S. Graham, Luc Piché, and Martin Grant, Phys. Rev. E **55**, 2132 (1997).
[6] S. M. M. R. Naqvi, S. D. H. Rizvi, S. M. Raza, A. Hussain, S. Rizvi, and F. Rehman, Solid State Commun. **10**, 479 (1998).
[7] J.-B. Suck, J. Non-Cryst. Solids **205-207**, 592 (1996).
[8] Z. Altounian, E. Batalla, J. O. Ström-Olsen, and J. L. Walter, J. Appl. Phys. **61**, 149 (1987).
[9] M. Dikeakos and Z. Altounian, J. Non-Cryst. Solids **250-252**, 786 (1999).
[10] M. Dikeakos, Ph.D. thesis, McGill University, 2002.
[11] T. Takeuchi and U. Mizutani, Phys. Rev. B **52**, 9300 (1994).
[12] U. Mizutani, Mater. Sci. Eng., A **294-296**, 464 (2000).
[13] R. Tamura, T. Araki, and S. Takeuchi, Phys. Rev. Lett. **90**, 226401 (2003).
[14] S. Banerjee, R. Goswami, K. Chattopadhyay, and A. K. Raychaudhuri, Phys. Rev. B **52**, 3220 (1995).
[15] Z. Altounian, S. V. Dantu, and M. Dikeakos, Phys. Rev. B **49**, 8621 (1994).
[16] U. Mizutani, *Rapidly Quenched Metals V*, edited by S. Steeb and H. Warlimont (Elsevier, New York, 1985), Vol. 1, p. 977.
[17] U. Mizutani, Prog. Mater. Sci. **28**, 97 (1983).
[18] U. Mizutani, *Rapidly Quenched Metals 6*, edited by R. W. Cochrane and J. O. Ström-Olsen (Elsevier, New York, 1988), Vol. 3, p. 165.
[19] Z. Altounian, C. A. Volkert, and J. O. Ström-Olsen, J. Appl. Phys. **57**, 1777 (1985).
[20] R. W. Tank, O. Jepsen, A. Burkhardt, and O. K. Andersen, *The Stuttgart TB-LMTO-ASA Program Version 4.7* (Max Planck Institut für Festköperforschung, Stuttgart, Germany, 1994).
[21] O. K. Andersen, O. Jepsen, and M. Sob, *Electronic Band Structure and Its Applications*, edited by M. Yussouff, Lecture Notes in Physics Vol. 283 (Springer-Verlag, New York, 1986), p. 1.
[22] O. K. Andersen, *The Electronic Structure of Complex Systems*, edited by P. Phariseau and W. M. Temmerman (Plenum Press, New York, 1984), p. 11.
[23] J. M. Mooij, Phys. Status Solidi A **17**, 521 (1973).